Fermi National Accelerator Laboratory

FERMILAB-Pub-98/403-E
KTeV E832/E799

Observation of the Decay $\Xi^0 \to \Sigma^+ \mathbf{e}^- \bar{\nu}_e$

A. Affolder et al.
The KTeV E832/E799 Collaboration

Fermi National Accelerator Laboratory
P.O. Box 500, Batavia, Illinois 60510

January 1999

Submitted to *Physical Review Letters*

Operated by Universities Research Association Inc. under Contract No. DE-AC02-76CH03000 with the United States Department of Energy

Disclaimer

This report was prepared as an account of work sponsored by an agency of the United States Government. Neither the United States Government nor any agency thereof, nor any of their employees, makes any warranty, expressed or implied, or assumes any legal liability or responsibility for the accuracy, completeness, or usefulness of any information, apparatus, product, or process disclosed, or represents that its use would not infringe privately owned rights. Reference herein to any specific commercial product, process, or service by trade name, trademark, manufacturer, or otherwise, does not necessarily constitute or imply its endorsement, recommendation, or favoring by the United States Government or any agency thereof. The views and opinions of authors expressed herein do not necessarily state or reflect those of the United States Government or any agency thereof.

Distribution

Approved for public release; further dissemination unlimited.

Copyright Notification

This manuscript has been authored by Universities Research Association, Inc. under contract No. DE-AC02-76CHO3000 with the U.S. Department of Energy. The United States Government and the publisher, by accepting the article for publication, acknowledges that the United States Government retains a nonexclusive, paid-up, irrevocable, worldwide license to publish or reproduce the published form of this manuscript, or allow others to do so, for United States Government Purposes.

FERMILAB-Pub-98/403-E

Observation of the Decay $\Xi^0 \to \Sigma^+ e^- \overline{\nu}_e$

A. Affolder[4], A. Alavi-Harati[12], I.F. Albuquerque[10], T. Alexopoulos[12], M. Arenton[11], K. Arisaka[2], S. Averitte[10], A.R. Barker[5], L. Bellantoni[7], A. Bellavance[9], J. Belz[10], R. Ben-David[7], D.R. Bergman[10], E. Blucher[4], G.J. Bock[7], C. Bown[4], S. Bright[4], E. Cheu[1], S. Childress[7], R. Coleman[7], M.D. Corcoran[9], G. Corti[11], B. Cox[11], M.B. Crisler[7], A.R. Erwin[12], R. Ford[7], A. Golossanov[11], G. Graham[4], J. Graham[4], K. Hagan[11], E. Halkiadakis[10], K. Hanagaki[8], S. Hidaka[8], Y.B. Hsiung[7], V. Jejer[11], J. Jennings[2], D.A. Jensen[7], R. Kessler[4], H.G.E. Kobrak[3], J. LaDue[5], A. Lath[10], A. Ledovskoy[11], P.L. McBride[7], A.P. McManus[11], P. Mikelsons[5], E. Monnier[4,*,†], T. Nakaya[7], U. Nauenberg[5], K.S. Nelson[11], H. Nguyen[7], V. O'Dell[7], M. Pang[7], R. Pordes[7], V. Prasad[4], C. Qiao[4], B. Quinn[4], E.J. Ramberg[7], R.E. Ray[7], A. Roodman[4], M. Sadamoto[8], S. Schnetzer[10], K. Senyo[8], P. Shanahan[7], P.S. Shawhan[4], W. Slater[2], N. Solomey[4], S.V. Somalwar[10], R.L. Stone[10], I. Suzuki[8], E.C. Swallow[4,6], R.A. Swanson[3], S.A. Taegar[1], R.J. Tesarek[10], G.B. Thomson[10], P.A. Toale[5], A. Tripathi[2], R. Tschirhart[7], Y.W. Wah[4], J. Wang[1], H.B. White[7], J. Whitmore[7], B. Winstein[4], R. Winston[4], J.Y. Wu[5], T. Yamanaka[8], E.D. Zimmerman[4]
(KTeV Collaboration)

[1] *University of Arizona, Tucson, Arizona 85721*
[2] *University of California at Los Angeles, Los Angeles, California 90095*
[3] *University of California at San Diego, La Jolla, California 92093*
[4] *The Enrico Fermi Institute, The University of Chicago, Chicago, Illinois 60637*
[5] *University of Colorado, Boulder, Colorado 80309*
[6] *Elmhurst College, Elmhurst, Illinois 60126*
[7] *Fermi National Accelerator Laboratory, Batavia, Illinois 60510*
[8] *Osaka University, Toyonaka, Osaka 560 Japan*
[9] *Rice University, Houston, Texas 77005*
[10] *Rutgers University, Piscataway, New Jersey 08855*
[11] *The Department of Physics and Institute of Nuclear and Particle Physics, University of Virginia, Charlottesville, Virginia 22901*
[12] *University of Wisconsin, Madison, Wisconsin 53706*

We present the first observation of Ξ^0 beta decay, using the KTeV beam line and detector at Fermilab. We have identified 176 beta decay events after subtracting a 7 event background. Normalization to 41 024 simultaneously collected $\Xi^0 \to \Lambda^0 \pi^0$ decays yields a branching ratio of $\Gamma(\Xi^0 \to \Sigma^+ e^- \overline{\nu}_e)/\Gamma_{\rm total} = (2.71 \pm 0.22_{\rm statistical} \pm 0.31_{\rm systematic}) \times 10^{-4}$. The flavor symmetric quark model calculation agrees with this result.

PACS numbers: 13.30.Ce, 14.20.Jn

(Submited to Physical Review letters on December 22, 1998)

We report the first observation of Ξ^0 beta decay, $\Xi^0 \to \Sigma^+ e^- \overline{\nu}_e$, and measurement of its branching ratio (BR). Under d and s quark interchange, this process is the direct analogue of the neutron beta decay, $n \to p e^- \overline{\nu}_e$. Thus, in the flavor symmetric quark model, differences between these two decays arise only from the differing particle masses and from the relevant Cabibbo Kobayashi Maskawa [1] matrix elements (V_{us} rather than V_{ud}). In the symmetry limit, the calculated [4] branching ratio is $(2.61 \pm 0.11) \times 10^{-4}$. Flavor symmetry violation effects [2,3] are expected to modify this branching ratio by several percent. The directly-measurable final state Σ^+ polarization should allow future precision measurements of form factors, providing additional information on flavor symmetry.

The KTeV beam line and detector at Fermilab were designed [5] for high precision studies of CP violation in the neutral kaon system (E832) and of rare decays (E799-II). Since the apparatus was situated far from the production target, to reduce backgrounds to K_L decays, only the highest momentum hyperons (130 to 600 GeV/c for Ξ^0 centered at 280 GeV/c) reached it. An intense neutral beam, powerful particle identification, and very good resolution for both charged particles and photons made it a good facility for the study of Ξ^0 decays. During data taking, about 5×10^6 Ξ^0 arrived at the decay volume each day. The data presented here were collected during two months of E799-II data-taking in 1997 and correspond to 20 % of all the hyperon data taken in 1997.

An 800 GeV/c proton beam, with up to 5×10^{12} protons per 19 s Tevatron spill every minute, was targeted at a vertical angle of 4.8 mrad on a 1.1 interaction length (30 cm) BeO target. Photons were converted by 7.6 cm of lead immediately downstream of the target. Charged particles were removed further downstream by dipole magnets. Collimators defined two 0.25 μsr neutral beams that entered the KTeV apparatus (Fig. 1) 94 m downstream from the target. The 65 m vacuum ($\sim 10^{-6}$ Torr) decay region extended to the first drift chamber.

The charged particle spectrometer consisted of a dipole

magnet surrounded by four (1.28×1.28 m^2 to 1.77×1.77 m^2) drift chambers (DC1–4) with ~100 μm position resolution in both horizontal and vertical views. To reduce multiple scattering, helium filled bags occupied the spaces between the drift chambers. In E799-II, the magnetic field imparted a ± 205 MeV/c horizontal momentum component to charged particles, yielding a momentum resolution of $\sigma(P)/P = 0.38\% \oplus 0.016\%\ P\,(\mathrm{GeV}/c)$. The magnet polarity was flipped on a daily basis.

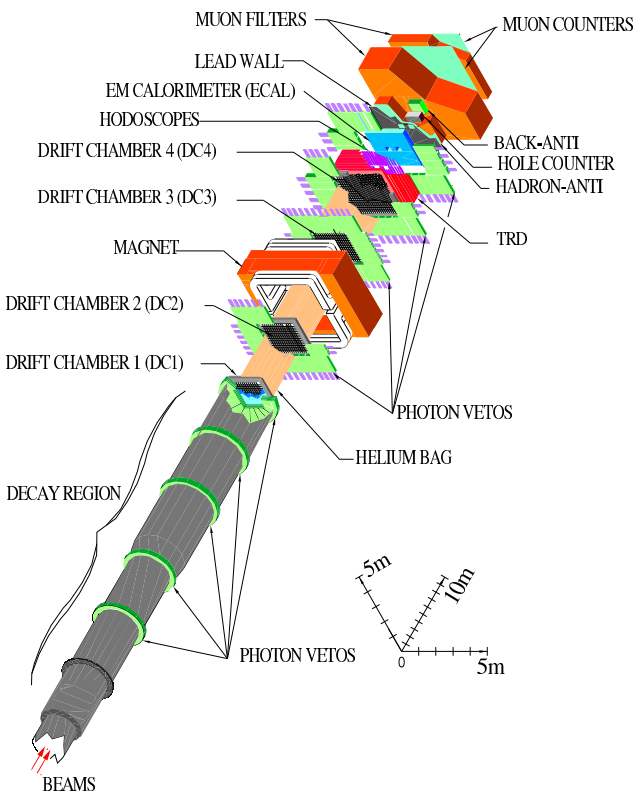

FIG. 1. The KTeV apparatus as configured for this measurement. The TRD, Muon and Back-Anti systems are not used in this analysis.

The electromagnetic calorimeter (ECAL) consisted of 3100 pure CsI crystals. Each crystal was 50 cm long (27 radiation lengths, 1.4 interaction lengths). Crystals in the central region (1.2×1.2 m^2) had a cross-sectional area of 2.5×2.5 cm^2; those in the outer region (1.9×1.9 m^2), 5×5 cm^2. After calibration, the ECAL energy resolution was 0.85% for the electron momentum spectrum in this analysis. The position resolution was ~1 mm.

Nine photon veto assemblies detected particles leaving the fiducial volume. Two scintillator hodoscopes in front of the ECAL were used to trigger on charged particles. Another scintillator plane (hadron-anti), located behind both the ECAL and a 10 cm lead wall, acted as a hadron shower veto. The hodoscopes and the ECAL detectors had two holes (15×15 cm^2 at the ECAL) and the hadron-anti had a single 64×34 cm^2 hole to let the neutral beams pass through without interaction. Charged particles passing through these holes were detected by 16×16 cm^2 scintillators (hole counters) located along each beam line in the hole region just downstream of the hadron-anti.

The beta decay, $\Xi^0 \to \Sigma^+ e^- \overline{\nu}_e$ followed by $\Sigma^+ \to p\pi^0$, has a topology similar to the dominant Ξ^0 decay sequence, $\Xi^0 \to \Lambda^0 \pi^0$ followed by $\Lambda^0 \to p\pi^-$, which was used for normalization. Both sequences had a high momentum (>100 GeV/c) positive track (proton) which remained in or near the neutral beam region, a second lower momentum negative track (π^- or e^-), and two neutral (*i.e.* unassociated to any track) ECAL energy clusters (photons from a π^0). The beta decay was distinguished by the presence of a decay electron and by its different vertex structure.

The basic hyperon trigger thus required a signal in one of the hole counters with corresponding signals from DC1 and DC2, one or more hodoscope signals, and no activity in the photon veto system. A special hardware stiff track trigger (STT) was used to select high momentum (>50 GeV/c) tracks based on hit positions in the DC1–4 horizontal views. This normalization mode trigger, prescaled by 50, provided our $\Xi^0 \to \Lambda^0 \pi^0$ candidates. The beta decay trigger, in addition to the hyperon trigger criteria, further required one to four in-time (within a 19 ns wide time slice) energy clusters [6] with a total energy of at least 18 GeV in the ECAL, minimal hadronic shower activity in the hadron-anti (< 2.5 times the minimum ionizing particle energy) and hits in the DC1–4 vertical views consistent with two tracks. The beta trigger was prescaled by 2. Finally, to allow studies of the hyperon trigger and of the beta trigger, there was a minimum bias trigger, prescaled by 20 000, that required only signals in the hodoscopes and in the hole counters.

In contrast to other hyperon beta decays, the absence of a competing two-body decay containing a Σ^+ eliminated a major background to our signal. Therefore, the possible backgrounds were: (a) $K_L^0 \to \pi^\pm e^\mp \nu_e$, $\Lambda^0 \to p\pi^-$, $\Lambda^0 \to p e^- \overline{\nu}_e$ decays with two accidental photons; (b) $K_L^0 \to \pi^0 \pi^\pm e^\mp \nu_e$, $K_L^0 \to \pi^+ \pi^- \pi^0$; and (c) $\Xi^0 \to \Lambda^0 \pi^0$ with either $\Lambda^0 \to p\pi^-$ or $\Lambda^0 \to p e^- \overline{\nu}_e$ as subsequent decays. As described below, clustering, kinematic and event topology selections strongly suppressed these backgrounds. The primary residual background was $\Xi^0 \to \Lambda^0 \pi^0$ followed by $\Lambda^0 \to p +$ anything. Background investigations and acceptance calculations were carried out with a detailed Monte Carlo simulation of the beam and detector.

During reconstruction and analysis, we sought to minimize event losses and to treat beta and $\Lambda^0 \pi^0$ candidates as similarly as possible. All events were required to have at least two neutral ECAL clusters (π^0 candidate) above 3 GeV and separated by more than 15 cm and a low momentum negative track (2.5–50 GeV/c for e^- and 2.5–75 GeV/c for π^-) pointing outside of the beam hole re-

gions of the ECAL. The proton was identified by a high momentum (110–400 GeV/c) positive track pointing to one of the beam holes of the ECAL. To reject K^0 backgrounds the positive over negative track momentum ratio was required to be greater than 3.5. Identical track quality and fiducial requirements were imposed on all events.

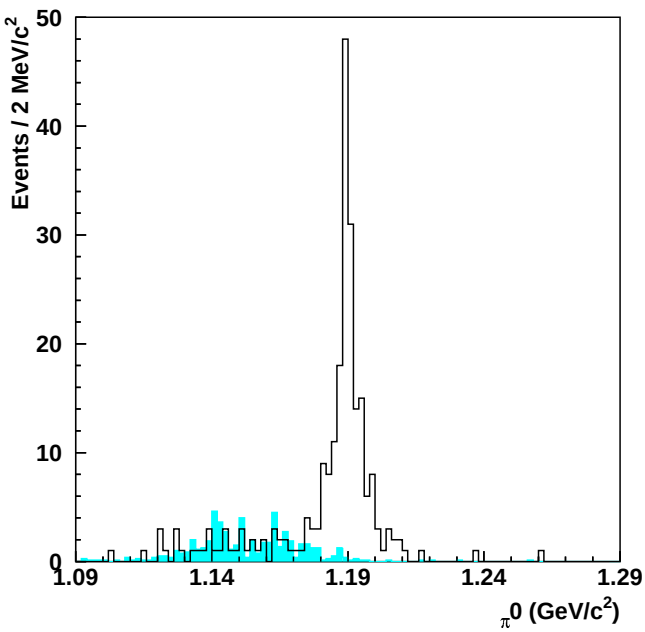

FIG. 2. Reconstructed $p\pi^0$ invariant mass distribution for the Ξ^0 beta decay candidates. Superimposed in gray is the simulated background from $\Xi^0 \to \Lambda^0\pi^0$ decays with $\Lambda^0 \to p$ + anything.

Candidate $\Xi^0 \to \Sigma^+ e^- \overline{\nu}_e$ reconstruction proceeded from downstream to upstream. The secondary Σ^+ decay vertex was located at the point along the proton track where the two highest energy neutral ECAL clusters matched the π^0 mass. The primary Ξ^0 vertex was then defined at the point of closest approach of the extrapolated Σ^+ path and the negative track. To remove $\Xi^0 \to \Lambda^0\pi^0$ background candidates, a $\Xi^0 \to \Lambda^0\pi^0$ hypothesis, described below, was used to reject candidates with a reconstructed $\Lambda^0\pi^0$ mass below 1.33 GeV/c^2.

All vertices were required to fall within the decay region fiducial volume (95-150 m), and primary Ξ^0 vertices were required to lie within a neutral beam. We eliminated primary Λ^0 or K^0 two-body decays by rejecting events with charged vertex transverse momentum squared less than 0.001 (GeV/c)^2. To enforce correct vertex geometry and to reduce further the primary Λ^0 or K^0 decay backgrounds, each secondary vertex was required to be 1–20 m downstream of the primary vertex. Further requirements were imposed on reconstructed Ξ^0 momentum (160–500 GeV/c) and decay distance ($<$ 10 lifetimes).

Only those events in the beta trigger sample which contain an e^-, identified by the deposition of more than 90% of its energy in the ECAL, were retained. We also required a suitable $\Sigma^+ e^-$ invariant mass (1.20–1.32 GeV/c^2) and a missing transverse momentum which was (within a 25 MeV/c uncertainty) less than the reconstructed neutrino momentum in the Ξ^0 rest frame.

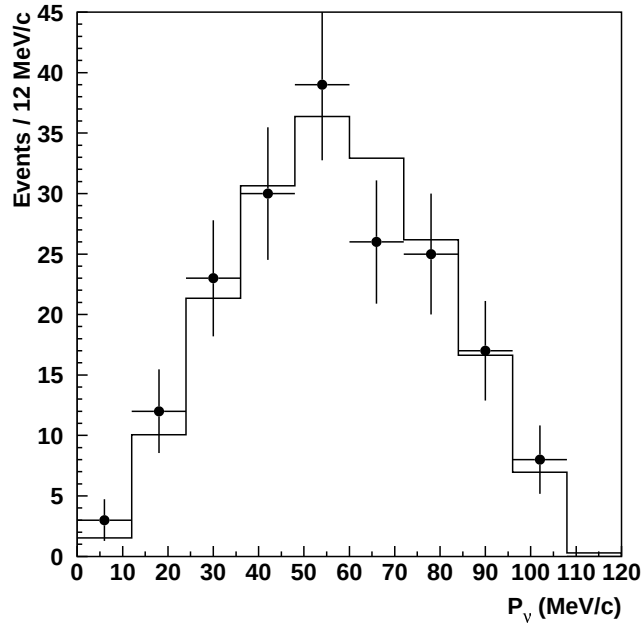

FIG. 3. Neutrino momentum spectrum in the Ξ^0 rest frame. Points are data with statistical uncertainties, and the histogram is our Monte Carlo simulation normalized to the same number of events. The acceptance has little effect on this distribution. The shape of the spectrum is typical of a beta decay.

The $p\pi^0$ invariant mass distribution for the 235 remaining candidates is shown in Fig. 2. A clear Σ^+ mass peak is apparent, containing 183 events within ± 15 MeV/c^2 (± 3 standard deviations) of the Σ^+ mass [7]. The gray region of Fig. 2 is the distribution for the primary predicted background, from Ξ^0 decay, normalized to the beam flux. The tail of this distribution was estimated to contribute 7 events under the mass peak. After subtracting this known background from the mass distribution, the residual background was estimated to be negligible by counting events in two 15 MeV/c^2 mass regions on either side of the peak (1.155-1.170;1.21-1.225) yielding a total sample of 176 ± 14 $\Xi^0 \to \Sigma^+ e^- \overline{\nu}_e$ events. The reconstructed Σ^+ and Ξ^0 decay distance distributions matched those predicted from known lifetime values. Distributions such as the proton and electron momentum spectra in the laboratory frame and the neutrino momentum spectrum in the Ξ^0 rest frame (Fig. 3) for simulated $\Xi^0 \to \Sigma^+ e^- \overline{\nu}_e$ decays all agreed with the data.

The $\Xi^0 \to \Lambda^0\pi^0$ candidate events were similarly identified in the hyperon trigger sample with a $\Xi^0 \to \Lambda^0\pi^0$ hypothesis. The two charged tracks were fit to locate the Λ^0 vertex. The reconstructed Λ^0 mass was

required to be within ± 10 MeV/c^2 (± 5 standard deviations) of its value [7]. The primary Ξ^0 decay vertex was then located along the extrapolated Λ^0 path using the π^0 constraint. Accepted events were required to have less than 80% of the negative track (π^-) energy deposited in the ECAL and to have a $\Lambda^0\pi^0$ invariant mass within ± 15 MeV/c^2 (± 5 standard deviations) of the Ξ^0 mass [7]. The resulting normalization sample contained 41 024 $\Xi^0 \to \Lambda^0\pi^0$ events. Again, kinematic distributions for simulated events agreed well with the data. The level of background in this sample was negligible.

Events from the minimum bias trigger and from the basic hyperon trigger were used to determine the beta and the basic hyperon trigger efficiencies and to validate aspects of the simulation. For the trigger elements unique to the beta trigger, a combined efficiency of $\epsilon = 0.98 \pm 0.01$ was obtained. For the trigger elements common to both triggers, only the STT had significant potential to create non-canceling effects. These effects arose because the DC wires used by the STT were the limiting aperture for protons and because the STT rejected events with more than one particle hitting these wires. We compared $\Lambda^0 \to p\pi^-$ and $\Xi^0 \to \Lambda^0\pi^0$ minimum bias trigger events with a Monte Carlo simulation. The STT absolute efficiency was 31 ± 3 % and its relative acceptance was 1.0 ± 0.1. We thus included a 10% systematic uncertainty contribution for the STT. When each of the selection criteria was systematically varied, no statistically significant variations were detected. We also found that the beta decay acceptance had a negligible dependence on the form factor values used in the simulation. We therefore assigned a combined 5% systematic uncertainty to our simulation of the relative acceptance. We also ascribed a ± 3 events systematic uncertainty to the background subtraction to allow for possible inadequacies in the subtraction method. Combined in quadrature, these contributions yielded a 11.3% net systematic uncertainty.

Monte Carlo studies gave a relative acceptance of $\epsilon \times \mathrm{A}(\Xi^0 \to \Sigma^+ e^- \overline{\nu}_e)/\mathrm{A}(\Xi^0 \to \Lambda^0\pi^0) = 0.98 \times 0.0253/0.0318 = 0.780 \pm 0.011_{\mathrm{stat.}} \pm 0.088_{\mathrm{syst.}}$. This includes losses due to detector geometry, trigger efficiencies, event reconstruction and particle identification with their corresponding statistical and systematic uncertainties. Using this relative acceptance, the two event samples with their prescale factors, and known branching ratios [7], we found $BR(\Xi^0 \to \Sigma^+ e^- \overline{\nu}_e) = \Gamma(\Xi^0 \to \Sigma^+ e^- \overline{\nu}_e)/\Gamma_{\mathrm{total}} = (2.71 \pm 0.22 \pm 0.31) \times 10^{-4}$. The first uncertainty is statistical and the second is systematic. As a further global test, we calculated BR values separately for each beam, for each analysis magnet polarity, and for the early and later halves of the data taking. In every case, the results were statistically consistent.

In summary, we observed Ξ^0 beta decay for the first time and measured its branching fraction. The clean beta decay signal (~4% total background) implies that we have suppressed the dominant Ξ^0 decay mode by more than 10^5. This branching ratio result does not distinguish between the exact flavor symmetry calculation and lower values based on flavor symmetry violation analyses [2,8]. We have now accumulated five times more events with improved triggering and systematic uncertainties, making possible future studies of decay angular distributions as well as a more accurate branching ratio determination that may distinguish between models.

We thank A. Garcia, A. Manohar, and J. Rosner for many helpful discussions. We gratefully acknowledge the support and effort of the Fermilab staff and the technical staffs of the participating institutions for their vital contributions. This work was supported in part by the U.S. Department of Energy, The National Science Foundation and The Ministry of Education and Science of Japan. In addition, A.R.B., E.B. and S.V.S. acknowledge support from the NYI program of the NSF; A.R.B. and E.B. from the Alfred P. Sloan Foundation; E.B. from the OJI program of the DOE; K.H., T.N. and M.S. from the Japan Society for the Promotion of Science. P.S.S. acknowledges receipt of a Grainger Fellowship.

---

* On leave from C.P.P. Marseille/C.N.R.S., France.
† To whom correspondence should be addressed. Electronic address: monnier@hep.uchicago.edu

[1] N. Cabibbo, Phys. Rev. Lett. **10**, 531 (1963) and M. Kobayashi and T. Maskawa Prog. Theor. Phys. **49**, 652 (1973). See also M. Gell-Mann and M. Levy, Nuovo Cimento **16**, 705 (1960) and Z. Maki, M. Nakagawa, and S. Sakata, Prog. Theor. Phys. **28**, 870 (1962).

[2] See, for example, R. Flores-Mendieta, E. Jenkins, and A. V. Manohar, Phys. Rev. D **58**, 094028 (1998); A. Garcia, R. Huerta, and P. Kielanowski, Phys. Rev. D **45**, 879 (1992); C. Avenarius, Phys. Lett. B **272**, 71 (1991); M. Roos, Phys. Lett. B **246**, 179 (1990); P. G. Ratcliffe, Phys. Lett. B **365**, 383 (1996); L. J. Carson, R. J. Oakes, and C. R. Willcox, Phys. Rev.D **37**, 3197 (1988) wherein flavor symmetry violation is considered in a variety of contexts.

[3] A. Garcia and P. Kielanowski, *The Beta Decay of Hyperons* (Lecture Notes in Physics, **222**, Springer–Verlag, 1985).

[4] We have used numerical values from reference [7] and the notation and formulae of reference [3] for this calculation ($f_1 = 1, |V_{us}| = 0.2196 \pm 0.0023$, $g_1/f_1 = 1.2670 \pm 0.0035$, $f_2/f_1 = 2.60$, $g_2 = 0$, $M_V = 970\,MeV/c^2$, $M_A = 1250\,MeV/c^2$). The uncertainties come primarily from the Ξ^0 mass and lifetime.

[5] K. Arisaka *et al.*, *KTeV (Kaons at the Tevatron) Design Report*, Fermilab Report No. FN-580, 1992.

[6] C. Bown *et al.*, Nucl. Instrum. Meth. A **369**, 248 (1996).

[7] Particle Data Group, C. Caso *et al.*, Eur. Phys. J. C **3**, 1 (1998).

[8] A. Manohar and A. Garcia, private communication.